Received: 23 February 2023 | Revised: 8 August 2023 | Accepted: 9 August 2023
DOI: 10.1002/qua.27222

RESEARCH ARTICLE

International Journal of QUANTUM CHEMISTRY WILEY

Bond dissociation energies of the fifth-row elements (In—I): A quantum theoretical benchmark study

Ismail Badran[1] | Kotaybah Hashlamoun[2] | Nashaat N. Nassar[2]

[1]Department of Chemistry, Faculty of Sciences, An-Najah National University, Nablus, Palestine

[2]Department of Chemical and Petroleum Engineering, University of Calgary, Calgary, Alberta, Canada

Correspondence
Ismail Badran, Department of Chemistry, Faculty of Sciences, An-Najah National University, Nablus, Palestine.
Email: i.badran@najah.edu

Funding information
Natural Sciences and Engineering Research Council of Canada

Abstract

The bond dissociation energies (BDE) of most main-group elements have been accurately measured. However, the BDE values for heavy elements, particularly those from the fifth period (In—I), are still missing or poorly validated. This study aims to identify the most accurate computational methods for calculating BDE values of compounds containing fifth-row elements, including In, Sn, Sb, Te, and I, with a focus on readily accessible methods in software packages. The investigation involved a benchmark study using density functional theory (DFT), in addition to the 2nd order Møller–Plesset perturbation theory (MP2) and the coupled cluster with single, double, and perturbative triple excitations CCSD(T). The DFT functionals used in the study include APFD, B3LYP, B3LYP-D3, B3P86, B97-D3, BHandH, HSEH1PBE, M06-2X, MN12-SX, MN15-L, and TPSSH. The functionals were carefully selected to cover some popular functionals as well as to cover all levels of the Jacob's ladder of DFT accuracy. The computed BDE values were compared with experimental values, and the results were filtered to remove any possible outliers. The statistical errors (MAPE, RMSE, and Pearson's) were then calculated and used to assess the performance of the methods.

KEYWORDS
benchmarking, bond dissociation energy, computational chemistry, DFT, fifth-row

1 | INTRODUCTION

The course of chemical and biological reactions is governed by the breaking and forming of chemical bonds. The bond dissociation energy (BDE) is a critical parameter for studying such reactions. Accurate BDE values are essential not only for estimating the enthalpy of chemical reactions but also for constructing reaction mechanisms, determining thermodynamically favored reaction pathways, and studying reaction kinetics [1–4]. Additionally, BDE's play a critical role in chemistry [5–7], Physics [8, 9], and biology [10–12], as they can be used to estimate the activation energy (a kinetic property) from the reaction enthalpy (a thermodynamic property) [13, 14].

Experimental determination of BDE for simple organic compounds is relatively straightforward, and BDE values of common representative elements (e.g., H, C, N, O, and S) have been experimentally determined with a great accuracy [15]. However, determining BDE for complex systems and molecules with heavy elements is rather challenging. Recent advances in computational methods have not only helped in validating experimental BDE values, but also in obtaining BDE for systems that cannot be studied experimentally [4]. Various different computational methods have been used to estimate and validate BDE values. These methods include configuration interaction (CI), 2nd order Møller–Plesset perturbation theory (MP2), coupled cluster (CC), and density functional theory (DFT) [16, 17]. These methods address the electron correlation problem to varying degrees, with some performing better than others. Typically, BDE are calculated by optimizing the chemical species involved in the bond breaking and then calculating their single-point energies. The BDE can then be obtained from the difference between the energy of the stable molecule and that of the individual free radicals or ions (with few corrections).

In ab-initio calculations, it is important to consider the method's size consistency; a property that guarantees the energy of a system (A + B) is equal to the sum of the energy of A plus that of B [18]. Some methods, such as pure CI, are not size consistent, while both MP2 and CCSD(T) are generally considered size consistent, and they were trusted by the computational community. However, MP2 was shown to overestimate the bond strength, particularly in transition metal complexes and some Si-containing structures, and therefore producing lower BDE [19, 20]. Similarly, the performance of CC methods in determining BDE has been recently criticized [3, 21, 22]. Although certain recent improvements to the CC and MP2 methods have been made to improve their accuracy, these adjustments are not available in all software packages and their use is still limited [23, 24]. Therefore, the performance of the pure MP2 and CC methods—which are still wildly used—needs continuous assessment.

Generally, DFT methods have shown excellent performance in determining BDE values for almost all molecular structures. The major problem of DFT, however, is that an exact exchange-correlation functional is still unknown [25, 26]. As a result, considerable efforts were made either to develop or to improve DFT functionals. The expansion and commercialization of computational software packages have made DFT even more popular. Unfortunately, the expansion of DFT came with a price. The use of DFT by non-experts has introduced significant discrepancies in the chemical literature; a situation that was described by some experts as the "DFT Zoo" [27, 28]. Consequently, some DFT functionals have been chosen for use in chemical problems based on their popularity rather than their accuracy [29].

In early 2000s, Perdew et al. proposed a hierarchy (Jacob's ladder, Figure 1) to classify DFT methods [30]. Starting from the Hartree-Fock level, which lacks electron correlation, the ladder grows from the simple local spin density approximation (LSDA) into generalized gradient approximation (GGA), followed by meta-GGA, then hybrid-GGA, and finally with the double-hybrid-GGA being the most accurate [27, 31]. Several benchmarking studies have shown that the accuracy of DFT functionals has agreed well with the hierarchy of the Jacob's ladder. For instance, Mardirossian and Head-Gordon evaluated 200 DFT functionals and discovered that their accuracy in estimating the binding energies of small molecules had obeyed the order of Jacob's ladder [31].

One of the most popular DFT functionals is the B3LYP, a hybrid functional developed in the early 1990s by Stephens et al. [32]. In recent years, the performance of B3LYP was heavily criticized, particularly in reactions taking place in solutions (dispersion effects), or involving heavy elements with a large number of electrons. In a benchmarking study by Goerigk et al. [27], the authors did not recommend the use of B3LYP in studying the thermochemistry of main-group elements. Based on their results, the authors hoped to "inspire a change in the user community's perception of common DFT methods" [27]. According to Kruse et al., the weakness of B3LYP is primarily attributed to two factors: (a) the lack of London dispersion effects, a feature needed to describe long-range separations and solvated systems, and (b) the basis set superposition error (BSSE). [29] The deficiency of B3LYP becomes severe when the functional is used with a small basis set, such as 6-31G*. [29] The weakness of B3LYP in estimating reaction energies was also documented in other studies [33, 34]. Consequently, the performance of the popular B3LYP functional needs to be assessed against other DFT functionals and methods. The dispersion corrected DFT-D3 approach will be also examined using the B3LYP-D3 functional [29, 35].

One of the most successful DFT functionals are those developed by the Truhlar group, commonly known as the Minnesota functionals [1]. This group of functionals covers all levels of the Jacob's Ladder. Examples of the Minnesota group include MPWLYP1W (GGA), [30] MN15-L (meta NGA), [36] M06-2X (hybrid meta GGA), [37] and the MN12-SX (range-separated hybrid meta-NGA). [38] Several benchmarking studies have been recently made to assess the performance of these functionals. The studies were performed on large data sets of molecules and ions and targeted the computation of different properties such as binding energies, isomerization energies, ionization potentials and electron affinities, barrier heights, and bond dissociation energies. The Minnesota functionals have demonstrated excellent performance in most of the computations [1, 27, 29, 31, 39]. Researchers have also agreed on the need to use dispersion-corrected functionals for systems that involve charge-separated species, such as ions, or solvation [31, 34, 40].

The currently available literature demonstrates extensive effort on benchmarking of DFT-functionals. However, benchmarking on the BDE of the fifth-row elements is very scarce. Besides, most benchmarking studies use database sets that are restricted to small common organic molecules; limiting the diversity of BDE data [28]. As a result of the scarcity of computational work on these elements, this study focuses on the fifth-period p-block elements (e.g., In, Sn, Sb, Te, and I). Some of the BDE of these elements have been determined experimentally. However, the BDE have large discrepancies because the experiments were not well-verified, in that they were only performed once, or were reported with a large standard error deviation. For example, the BDE energy of In-F bond in In_2F was reported to be 370 ± 50 kJ/mol [41].

The goal of this study is to assess the performance of different computational methods in calculating the BDE of fifth-row main-group elements. A total of 11 DFT functional were chosen for this task; APFD, B3LYP, B3LYP-D3, B3P86, B97-D3, BHandH, HSEH1PBE, M06-2X, MN12-SX, MN15-L, and TPSSH. In addition, the study was also performed using MP2 and CCSD(T) methods to assess their performance. Because some BDE values are missing or poorly validated for some of the fifth-row elements, this work is also aimed at locating a trusted level of theory that can be used to calculate the BDE with confidence. The significance of this work is that it enables general DFT users in fields such as chemistry, engineering, and biology to determine the BDE of compounds containing these elements with high accuracy using readily accessible software at a low computational cost.

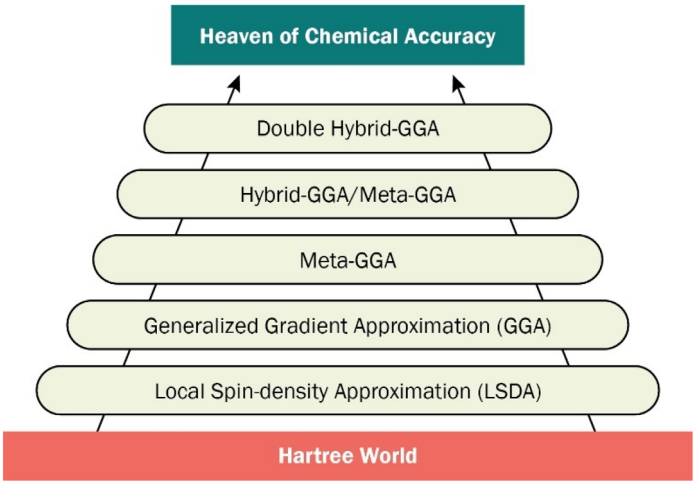

FIGURE 1 Jacob's ladder proposed by Perdew that classifies DFT functionals in increasing computational accuracy.

2 | COMPUTATIONAL METHODS

The methodology of this work involves three stages: (1) the BDE of a dataset of common organic compounds (e.g., H_2O, NH_3, and CH_3Cl) and molecules containing the elements (In, Sn, Sb, Te, and I) were calculated at different levels; (2) a statistical analysis was performed to exclude the outliers and obtain reliable error values; (3) the best computational methods were selected and used to calculate final BDE values.

In this work, the bond dissociation energy (BDE) is defined as the change of enthalpy at 298 K (ΔH_{298}) for the reaction, [41]

$$AB \rightarrow A + B \tag{1}$$

The enthalpy change (H_{298}) for a given species can be computed using ab-initio techniques as:

$$H_{298} = H_0 + H_{\text{corr.}} \tag{2}$$

where H_0 is the enthalpy change at 0 K and is defined as

$$H_0 = \text{SPE} + \text{ZPE}_{\text{scaled}} \tag{3}$$

where SPE is the single point energy and $\text{ZPE}_{\text{scaled}}$ is the scaled zero-point energy. The scaling was done according to Merrick et al. [42]. The correction to enthalpy ($H_{\text{corr.}}$) was obtained from frequency calculations after successful optimization for each specie. The unscaled ZPE was subtracted from ($H_{\text{corr.}}$) before the latter was added into Equation 2. The changes in Gibbs free energy (ΔG_{298}) have been also computed from enthalpy and ZPE corrections, and tabulated in a separate spreadsheet (See link https://www.doi.org/10.17632/vvbcfvwrzx.2) [19, 43, 44]. The calculations were done by requesting ground-state optimization for the species and the stable products of each reaction, followed by frequency calculations at the required method. Care was given to assign the most stable spin multiplicity for each specie based on the literature. The Pople's basis set 6-31+G(d,p) was used for light elements (H, C, N, O, F, and Cl). As for the heavy elements (In, Sn, Sb, Te, and I), the effective core potential (ECP) method was implemented using the Stuttgart/Dresden SDD basis set [45], and utilizing the (GEN) keyword in Gaussian. Both basis sets have demonstrated good performance in obtaining BDE values.

To ensure the accuracy of the basis set used [6-31+G(d,p)], a benchmark study was performed on a larger basis set [6-311++G(3d2f,2df,2p)] using the B3LYP functional. The use of the larger bases resulted in only minor improvements to the findings. In fact, a two-tailed *t*-test was run, and the *p*-value was found to be much greater than 5%. So there was no significant difference in the results obtained at the 6-31+G(d,p) and the 6-311++G(3d2f,2df,2p) basis sets. Therefore, the former was implemented to reduce computational costs.

A description of the methods used in this work is shown in Table 1. The functionals were carefully selected to be part of the study based on their previous performance, popularity, and such that they cover all levels in the Jacob's Ladder.

The study was performed on a total of 33 stable molecules. A total of 65 species were optimized in this study using the 13 level of theories shown in Table 1, leading to a total number of 780 single point calculations. All calculations were done using Gaussian 16 Rev C.01 [58] and viewed using Gaussview [59].

TABLE 1 Description of the computational methods used in this work.

Functional	Description	Classification	Ref.
APFD	Austin–Frisch–Petersson functional with dispersion	Local with dispersion	[46]
B3LYP	Becke's functional with the LYP expression	Hybrid GGA with no dispersion	[47]
B3LYP-D3	B3LYP with dispersion-correction functional	Hybrid GGA with dispersion	[47]
B3P86	Becke's functional with the non-local correlation	Hybrid GGA with no dispersion	[48]
B97-D3	Grimme's functional	Local GGA with dispersion	[49, 50]
BHandH	A mix of HF, LSDA, and LYP expressions	Hybrid GGA with no dispersion	[51]
HSEH1PBE	Heyd-Scuseria-Ernzerhof functional	Hybrid GGA with no dispersion	[52, 53]
M06-2X	Truhlar Minnesota functional	Hybrid meta GGA	[37]
MN12-SX	Truhlar Minnesota functional	Range-separated hybrid meta-NGA	[38]
MN15-L	Truhlar Minnesota functional	Meta nonseparable gradient approximation (meta-NGA)	[36]
TPSSh	A functional with a gradient-corrected correlation	Hybrid meta GGA with no dispersion	[9]
MP2	2nd order Møller–Plesset perturbation theory	Post–Hartree–Fock method	[54, 55]
CCSD(T)	Coupled cluster with single double, and perturbative triple excitations	Post–Hartree–Fock method	[56, 57]

The statistical analysis of the results was done as follows: First, the mean absolute percentage error (MAPE) was calculated by [60]:

$$\mathrm{MAPE} = \frac{100\%}{n} \sum_{i=1}^{n} \left| \frac{y_i - x_i}{y_i} \right| \tag{4}$$

where y_i and x_i are the experimental (reported) and calculated BDE values, respectively. The parameter n is the number of calculated values. The root-mean-square deviation (RMSE) was calculated by [7, 60, 61]:

$$\mathrm{RMSE} = \sum_{i=1}^{n} \frac{(y_i - x_i)}{n} \tag{5}$$

The standard deviation was calculated by [60]:

$$\sigma = \sqrt{\frac{\sum_{i=1}^{n} (x_i - \mathrm{MAPE})^2}{n}} \tag{6}$$

The Pearson's correlation (R) was calculated by [7, 60, 61]:

$$R = \frac{\sum_{i=1}^{n} (x_i - \overline{x})(y_i - \overline{y})}{\sqrt{(x_i - \overline{x})^2 (y_i - \overline{y})^2}} \tag{7}$$

As some errors produced from this work may be substantial, either due to erroneous experimental (reported) values, or due to the methods themselves, it is important to remove any outliers before calculating the final average error for each method. For the purpose of this study, the Z-score method was used. The Z-score for each calculated BDE value was obtained from the following equation [60]:

$$z_i = \frac{x_i - \mathrm{MAPE}}{\sigma} \tag{8}$$

The Z-score represents the number of standard deviations it is away from the mean. Data points with Z-scores above a certain threshold (commonly 2 or 3) are considered outliers [62, 63]. Thus, all BDE values in this work with Z-scores above three were first excluded. Then, the Z-scores were recalculated and BDE values with Z-scores larger than 1.95 were excluded. The final absolute errors for each model chemistry were recalculated and reported after excluding all outliers. The statistical and database analysis was done using Wolfram Mathematica [64].

3 | RESULTS AND DISCUSSION

Given the importance of the fifth-period representative elements, and the lack of validated data on their BDE, we employed quantum theoretical calculations to compute the BDE of these elements using different methods. The datasets of molecules used in this work are shown in Table 2. The broken bond is shown in the second column, with the *leaving* group marked with a dash. The first set (rows 1 to 7) is made of common compounds with well-documented BDE. The common compounds are CH_3CH_3, CH_3Cl, CH_3F, CH_3NO_2, H_2O, NH_3, PH_3, SF_6. $N(CH_3)_3$ and $SiH(CH_3)_3$. Because these molecules are well investigated in literature and their BDE values are well known, they assist us in examining the performance of the computational approaches under consideration. The rest of the table contains compounds of the fifth-row elements (In, Sn, Sb, Te, and I). The compounds were carefully selected to cover *two* types of bonding; M—M bonding (i.e., I—I, Te—Te, In—In, etc.), and M-X bonding, where X is a common light element such as H, C, O, F, and Cl. Only molecules with reported BDE values in the literature were selected.

As mentioned in the Introduction section, we selected a set of DFT functionals that cover different levels of the Jacob's ladder. In addition, our study was performed using MP2 and CCSD(T) methods to assess their performance in computing BDE for the fifth-period elements. Table 2 shows the calculated BDE values at different levels of theory. The experimental values obtained from the literature are also tabulated for reference. By examining the data in Table 2, we found that some calculated values deviate strongly from the reported value. The deviation was either correlated with the method (e.g., TPSSh, MP2, CCSD(T)), or with a specific molecule such as in the case of $InSb_2$, $SbCl_5$, and $TeCl_4$. To further investigate the deviations, the absolute percentage errors were calculated and tabulated in Table 3. As seen, some errors are considerably high (>30%). To better visualize the errors, Figure 2 shows the heat map of the data of Table 3. The data in Figure 2 were sorted based on the MAPE obtained for each molecule followed by the computational method. Most of the molecules used in this study show low to moderate MAPE as marked by their bluish colors in Figure 2. In contrast, some molecules deviate significantly from the experimental values (red and purple), and they are concentrated to the right of the figure. The worst MAPE were associated with the molecules: $TeCl_4$, $SbCl_5$, $InSb_2$, $Sb(CH_3)_5$, and ICl. Based on the heat map, we cannot rely on their reported BDE. Consequently, they were not considered in the subsequent statistical analysis. The heat map in Figure 2 also demonstrates the general performance of the computational methods used in this work. The figure suggests that the Minnesota DFT functionals, M06-2X, MN12-SX, and MN15-L are performing very well with low to moderate MAPE values. The enhanced B3P86 by Perdew is likewise among the top-performing functionals. It is unexpected that the "golden" methods, MP2 and CCSD(T), did not perform well in predicting the BDE of the molecules studied in this work, even for the most common and well-known small molecules. For instance, CCSD(T) predicts a BDE of 305.9 kJ/mol for the H_3C—Cl bond, which is 12.5% lower than reported value (377.4 kJ/mol). For phosphine (PH_3), the errors in predicting the BDE obtained at MP2 and CCSD(T) are 11.2% and 10.6%, respectively. The cause of this weak performance is discussed below.

To obtain the final MAPE for the BDE in this work, we conducted a statistical analysis to remove the outliers in Table 2 (cf. Section 2), all outliers with *Z*-score greater than 3.00 were eliminated first. The *Z*-scores were then recalculated, and outliers with *Z*-score exceeding 1.95 were removed. The remaining data were then used to obtain the final MAPE and RMSE. The results after removing the outliers are shown in Table 4. The blank fields represent the omitted outliers based on the above criterion. Overall, the BDE values obtained from all the methods are well correlated the reported values with Pearson's correlation (*R*) scores that exceeds 0.97, except that of MP2 (0.955). The final absolute percentage errors are also depicted in the heat map in Figure 3. In comparison with the previous heat map (Figure 2), the map is now more bluish indicating lower errors as a result of removing the outliers. The rustles from the CCSD(T) method have a MAPE of 10.0 ± 5.1%. The MP2 method has an estimated MAPE of 7.9 ± 6.2%. The relative weakness of MP2 and CCSD(T) in this particular study is also reflected by their large RMSE values of 39.8 and 41.0, respectively. The weak performance of MP2 and CCSD(T) comes as a surprise given that both methods are regarded as the "golden" paradigms of ab-initio techniques. The weakness of post-HF methods, such as MP2 and CCSD(T), in describing the hemolytic dissociation for complex systems might be attributed to two issues: (1) the basis set superposition error, and (2) the incomplete description of electron correlation [16, 22, 68]. The weak performance of these methods in this work might be due to their incomplete treatment of both components of the electronic correlation [16, 17, 22, 68]. Given that good treatment of electronic correlation is also needed for the close-lying electronic levels in the heavy elements of the fifth-period. The performance of both MP2 and CCSD(T) in this work is likewise consistent with some previous studies. By taking a closer look at Table 2, we found that the MP2 energies are mostly lower than experimental values. This can be explained by the fact that MP2 is known to underestimate the bond strength for some systems [19, 20]. A similar observation can be made for CCSD(T), which was also reported to underestimate BDE [3, 21, 22]. It is imperative to take into account that this work is subject to a limitation regarding the use of the 6-31+G (d,p) basis set. According to recent studies [69–71], the accuracy of MP2 and CCSD(T) methods can be highly influenced by the size and configuration of the basis set employed, as well as the neglection of relativistic effects. Thus, the choice of the 6-31+G(d,p) basis set in this study may impact the overall precision of the results.

In a study by Fang et al. [72], CCSD(T) demonstrated excellent performance in calculating the bond dissociation energies in M-H complexes, where M represents a 3rd-row transition metal. The authors attributed the good performance to the proper treatment of the basis set under the Complete Basis Set (CBS) approach, where the aug-ccpwCVnZ-DK basis set was used. However, in our study, we focus the elements of the fifth row (In—I) are larger and their electron structure is more complex. Thus, obtaining accurate BDE for such elements requires not only the proper treatment the basis set, but also the choice of the computational method.

TABLE 2 Experimental and calculated bond dissociation energy values obtained at different levels of theory.

Molecule and formula	The broken bond	Exp.	STD in exp.	APFD	B3LYP	B3LYP-D3	B3P86	B97-D3	BHandH	HSEH1PBE	M06-2X	MN12-SX	MN15-L	TPSSH	MP2	CCSD(T)
Ethane, CH_3CH_3	$H_3C—CH_3$	377.4 [15]	0.8	372.5	356.5	360.5	374.6	362.7	412.1	369.3	381.7	392.0	368.9	351.2	372.6	351.2
Chloromethane, CH_3Cl	$H_3C—Cl$	350.2 [15]	1.7	340.1	326.3	328.9	346.8	335.6	371.8	340.4	348.1	359.1	350.9	332.3	328.1	305.9
Fluoromethane, CH_3F	$H_3C—F$	460.2 [15]	8.4	448.3	447.6	449.7	462.2	461.8	482.6	446.5	459.5	469.9	455.6	444.6	459.9	424.4
Nitromethane, CH_3NO_2	$H_3C—NO_2$	260.7 [15]	2.1	246.1	233.7	239.6	250.8	230.4	301.7	246.5	266.6	281.9	250.9	226.8	252.7	237.5
Water, H_2O	HO—H	497.1 [15]	0.1	479.9	483.0	483.1	498.9	495.4	502.5	476.5	488.1	500.9	489.3	477.6	481.1	458.5
Ammonia, NH_3	$H_2N—H$	450.1 [15]	0.24	439.9	442.2	442.3	456.6	449.2	466.4	437.3	449.3	462.7	446.7	437.8	433.9	418.4
Phosphine, PH_3	$H_2P—H$	351.0 [15]	2.1	333.9	338.9	339.4	348.9	343.3	353.5	331.6	339.3	356.7	352.4	346.1	311.6	313.8
Sulfur hexafluorde, SF_6	$F_5S—F$	391.6 [15]	12.0	370.5	341.6	343.8	371.7	336.7	437.9	363.4	399.6	407.7	421.6	350.7	397.6	360.6
Trimethylamine, (TMA) $N(CH_3)_3$	$(CH_3)_2N—CH_3$	328.9 [15]	0.1	315.4	293.0	302.9	314.4	302.9	362.9	310.0	337.2	335.1	321.1	290.4	342.3	302.9
Trimethylsilane,TriMS, $SiH(CH_3)_3$), Me loss	$(CH_3)_2HSi—CH_3$	387.0 [15]	7.0	379.2	386.9	390.0	392.1	383.2	401.7	374.4	383.2	403.9	394.1	391.1	365.3	370.7
Trimethylsilane,TriMS, $SiH(CH_3)_3$), H loss	$(CH_3)_3Si—H$	396.2 [15]	4.2	363.0	348.0	355.5	361.8	349.3	401.6	357.4	371.6	391.3	368.7	344.8	365.7	349.3
Indium(III) hexafluoride, In_2F_6	$In_2F_5—F$	506.0 [41]	50.0	471.1	484.7	486.6	487.0	500.0	485.1	468.4	496.6	498.9	487.4	464.2	504.7	471.6
Indium(III) chloride, $InCl_3$	$InCl_2—Cl$	364.8 [15]	0.0	344.9	337.0	340.6	350.7	344.7	366.1	342.6	373.0	375.9	350.3	339.1	334.5	319.1
Indium trihydride, InH_3	$InH_2—H$	295.8 [15]	0.0	287.7	302.4	302.9	305.9	315.1	300.0	285.0	309.2	320.4	322.0	302.8	267.2	272.2
Trimethylindium, $In(CH_3)_3$	$(CH_3)_2In—CH_3$	269.0 [15]	0.0	259.3	254.3	257.9	264.8	264.1	283.4	256.1	294.8	292.2	265.1	247.6	255.7	245.5
Indium diantimonide, $InSb_2$	SbIn—Sb	279.1 [15]	0.0	198.5	189.5	190.1	211.6	251.6	183.1	200.5	217.5	162.8	185.9	186.7	117.6	104.1
Tin(IV) chloride, $SnCl_4$	$Cl_3Sn—Cl$	305.0 [15]	55.0	292.2	273.1	279.6	292.0	277.2	317.3	287.5	314.7	312.0	284.4	279.4	292.0	275.9
Stannane, SnH_4	$H_3Sn—H$	346.0 [15]	0.0	330.9	344.2	345.3	348.0	356.1	344.5	327.4	357.4	368.8	358.9	348.6	316.1	320.7
Tetramethylstannane, $Sn(CH_3)_4$	$(CH_3)_3Sn—CH_3$	295.0 [15]	17.0	271.5	259.1	265.0	271.9	268.2	298.2	265.9	301.0	304.1	269.9	254.3	273.5	260.1
Trimethylstannane, $Sn(CH_3)_3H$	$(CH_3)_3Sn—H$	326.4 [15]	0.0	305.5	314.6	316.1	320.8	319.2	321.9	301.8	325.5	333.6	325.6	317.3	288.4	295.3
Antimony(V) chloride, $SbCl_5$	$Cl_4Sb—Cl$	248.0 [65]	50.0	151.5	119.2	129.0	144.6	132.5	178.3	143.1	167.4	171.1	148.6	136.2	153.0	125.0
Stibine, SbH_3	$H_2Sb—H$	288.3 [15]	2.1	271.4	280.3	281.1	287.3	295.6	281.5	268.7	286.1	301.6	289.2	284.7	241.9	251.9
Pentamethyl stibine, $Sb(CH_3)_5$	$(CH_3)_4Sb—CH_3$	255.0 [66]	—	182.6	158.1	168.5	177.6	171.8	214.6	173.6	207.9	216.5	180.8	154.7	201.7	169.8
Ditellurium, Te_2	Te—Te	257.6 [15]	4.0	241.6	233.8	234.0	252.4	292.6	224.6	243.7	253.1	280.0	250.9	237.5	143.9	152.9
Tellurium(IV) chloride,$TeCl_4$	$TeCl_3—Cl$	310.0 [65]	—	150.2	130.9	143.9	154.1	169.1	129.0	147.0	132.7	159.7	149.5	145.5	140.8	90.8
Tellane, TeH_2	HTe—H	272.0 [15]	0.4	289.2	295.7	296.1	304.8	311.8	297.7	287.0	298.2	321.3	307.0	300.4	252.1	263.6
Dimethyltellane, $Te(CH_3)_2$	$CH_3Te—CH_3$	276.0 [67]	0.0	229.3	212.7	220.8	230.1	239.3	249.3	226.1	259.5	258.1	228.0	215.2	215.8	206.7
Iodane (Hydrogen iodide), HI	I—H	298.3 [15]	0.1	298.2	301.9	302.0	313.5	319.3	305.5	296.3	302.9	331.2	316.5	307.0	254.1	266.9
Iodine, I_2	I—I	152.3 [15]	0.6	128.6	118.7	119.1	134.6	149.7	126.0	130.7	141.1	179.8	144.3	129.6	62.6	84.4
Chloroiodomethane, ICH_2Cl	$I—CH_2Cl$	221.8 [15]		205.0	186.6	190.8	205.5	211.4	216.1	202.6	221.1	235.5	201.1	195.5	184.3	178.1

TABLE 2 (Continued)

Molecule and formula	The broken bond	Exp.	STD in exp.	APFD	B3LYP	B3LYP-D3	B3P86	B97-D3	BHandH	HSEH1PBE	M06-2X	MN12-SX	MN15-L	TPSSH	MP2	CCSD(T)
Iodine monochloride, ICl	I—Cl	211.3 [15]	0.4	167.0	157.9	158.1	174.7	178.7	172.5	167.9	176.9	200.4	170.1	171.8	125.1	125.5
Iodoformonitrile, ICN	I—CN	320.1 [15]	0.0	325.1	308.5	310.8	327.6	312.3	351.2	323.6	338.5	354.0	326.9	311.1	388.2	297.0
Iodine monofluoride, IF	I—F	271.5 [15]	0.0	238.7	244.7	244.8	254.2	268.5	246.0	237.5	253.8	273.9	248.8	246.8	261.2	232.9

TABLE 3 Row absolute percentage errors for the bond dissociation energies at different levels of theory, before excluding any outlier.

	APFD	B3LYP	B3LYP-D3	B3P86	B97-D3	BHandH	HSEH1PBE	M06-2X	MN12-SX	MN15-L	TPSSH	MP2	CCSD(T)
CH_3CH_3	1.3	5.5	4.5	0.7	3.9	9.2	2.1	1.1	3.9	2.2	6.9	1.3	7.0
CH_3Cl	2.9	6.8	6.1	1.0	4.2	6.2	2.8	0.6	2.6	0.2	5.1	6.3	12.7
CH_3F	2.6	2.7	2.3	0.4	0.3	4.9	3.0	0.1	2.1	1.0	3.4	0.1	7.8
CH_3NO_2	5.6	10.4	8.1	3.8	11.6	15.7	5.5	2.3	8.1	3.8	13.0	3.1	8.9
H_2O	3.5	2.8	2.8	0.4	0.3	1.1	4.1	1.8	0.8	1.6	3.9	3.2	7.8
NH_3	2.3	1.8	1.7	1.5	0.2	3.6	2.8	0.2	2.8	0.7	2.7	3.6	7.0
PH_3	4.9	3.5	3.3	0.6	2.2	0.7	5.5	3.3	1.6	0.4	1.4	11.2	10.6
SF_6	5.4	12.8	12.2	5.1	14.0	11.8	7.2	2.0	4.1	7.7	10.5	1.5	7.9
TMA	4.1	10.9	7.9	4.4	7.9	10.3	5.7	2.5	1.9	2.4	11.7	4.1	7.9
TriMS (Me loss)	2.0	0.0	0.8	1.3	1.0	3.8	3.3	1.0	4.4	1.8	1.1	5.6	4.2
TriMS (H loss)	8.4	12.2	10.3	8.7	11.8	1.4	9.8	6.2	1.2	6.9	13.0	7.7	11.8
In_2F_6	6.9	4.2	3.8	3.8	1.2	4.1	7.4	1.9	1.4	3.7	8.3	0.3	6.8
$InCl_3$	5.4	7.6	6.6	3.9	5.5	0.3	6.1	2.3	3.1	4.0	7.1	8.3	12.5
InH_3	2.7	2.2	2.4	3.4	6.5	1.4	3.7	4.5	8.3	8.9	2.4	9.7	8.0
$InMe_3$	3.6	5.5	4.1	1.6	1.8	5.4	4.8	9.6	8.6	1.4	7.9	5.0	8.7
$InSb_2$	28.9	32.1	31.9	24.2	9.8	34.4	28.2	22.1	41.7	33.4	33.1	57.9	62.7
$SnCl_4$	4.2	10.5	8.3	4.2	9.1	4.0	5.8	3.2	2.3	6.8	8.4	4.3	9.5
SnH_4	4.4	0.5	0.2	0.6	2.9	0.4	5.4	3.3	6.6	3.7	0.7	8.6	7.3
$SnMe_4$	8.0	12.2	10.2	7.8	9.1	1.1	9.9	2.0	3.1	8.5	13.8	7.3	11.8
SnTriMeH	6.4	3.6	3.2	1.7	2.2	1.4	7.5	0.3	2.2	0.2	2.8	11.6	9.5
$SbCl_5$	38.9	52.0	48.0	41.7	46.6	28.1	42.3	32.5	31.0	40.1	45.1	38.3	49.6
SbH_3	5.9	2.8	2.5	0.4	2.5	2.4	6.8	0.8	4.6	0.3	1.3	16.1	12.6
$SbMe_5$	28.4	38.0	33.9	30.4	32.6	15.9	31.9	18.5	15.1	29.1	39.3	20.9	33.4
Te_2	6.2	9.2	9.2	2.0	13.6	12.8	5.4	1.7	8.7	2.6	7.8	44.1	40.6
$TeCl_4$	51.5	57.8	53.6	50.3	45.5	58.4	52.6	57.2	48.5	51.8	53.1	54.6	70.7
TeH_2	6.3	8.7	8.9	12.0	14.6	9.5	5.5	9.6	18.1	12.9	10.5	7.3	3.1
$TeMe_2$	16.9	22.9	20.0	16.6	13.3	9.7	18.1	6.0	6.5	17.4	22.0	21.8	25.1
HI	0.0	1.2	1.2	5.1	7.0	2.4	0.6	1.6	11.0	6.1	2.9	14.8	10.5
I_2	15.5	22.1	21.8	11.6	1.7	17.3	14.1	7.3	18.1	5.2	14.9	58.9	44.6
ICH_2Cl	7.6	15.9	14.0	7.3	4.7	2.6	8.7	0.3	6.2	9.3	11.9	16.9	19.7
ICl	21.0	25.3	25.2	17.3	15.4	18.4	20.6	16.3	5.2	19.5	18.7	40.8	40.6
ICN	1.6	3.6	2.9	2.3	2.4	9.7	1.1	5.7	10.6	2.1	2.8	21.3	7.2
IF	12.1	9.9	9.9	6.4	1.1	9.4	12.5	6.5	0.9	8.4	9.1	3.8	14.2

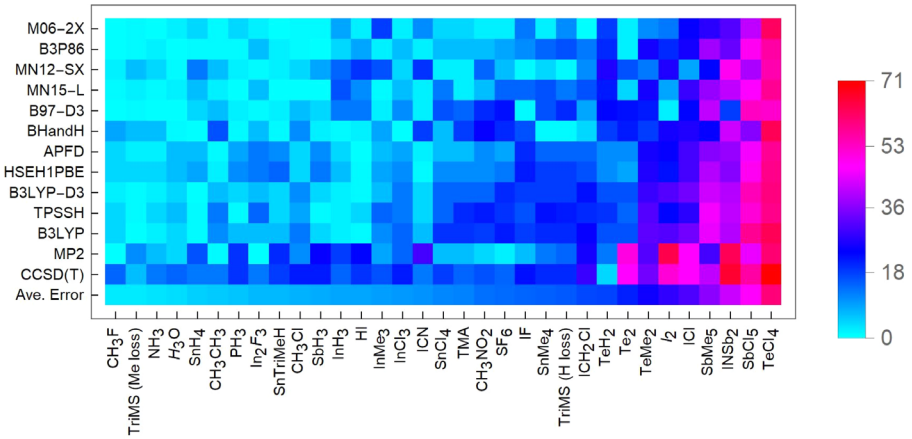

FIGURE 2 Row absolute percentage errors for the bond dissociation energies at different levels of theory, before excluding any outlier.

Because the pure HF approach fails to treat hemolytic bond dissociation, the BHandH functional may not perform very well. In this study, the MAPE of the BHandH functional was determined to be 5.0 ± 4.0%, which is inadequate. Even for common molecules, such as CH_3CH_3 and CH_3NO_2, the functional overestimates their BDE by 9.2% and 15.7%. The BHandH is a half-and-half functional that is made of 50% HF with 50% LSDA. The first is pure HF that completely lacks electron correlation, while the second is known to have weak accuracy in energy calculations, provided it is in the lowest level of the Jacob's ladder (cf. Figure 1) [7, 27, 31]. According to Moltved et al., the HF method is so pathological in energy calculations, even upon mixing with DFT functionals, such as BHandH [22].

As stated in the introduction, the popular B3LYP functional's performance has been heavily criticized [27, 29, 33, 34]. In this work, the estimated MAPE of the B3LYP was 6.4 ± 4.6%. The RMSE is also high at 27.2 even after exculduing outliers.

The functional's poor performance not only applies to compounds of heavy elements, but also to light ones with trusted experimental BDE values. As an example, the absolute errors obtained using B3LYP, for CH_3NO_2 (10.4%), ICH_2Cl (15.9%) and SF_6 (12.8%) cannot be accepted, given the basis set (6-31+G(d,p), SDD) used in this study. In addition, the discrepancies provided by the B3LYP functional is puzzling; for example, the methyl loss in TriMS is estimated at 386.9 kJ/mol (almost 0% error), while it is 348.0 kJ/mol with 12.2% error from the experimental value. Based on moderate performance of the B3LYP functional in this study, and the recent recommendations of other scholars [27, 29, 33], we insist that B3LYP should be used with caution to compute BDE of heavy elements.

In order to improve the results of B3LYP, we used the DFT-D3 approach through the B3LYP-D3 functional. The B3LYP-D3 performed slightly better than the B3LYP, but the difference was not significant. The MAPE values for B3LYP and B3LYP-D3 were 6.4 and 5.7, respectively. This is supported by the close values of the Pearson's correlations (0.976. 0.980) and the RMSE (27.2, 24.1) are B3LYP and B3LYP-D3, respectively. According to a study by Kruse et al. [29], the use of B3LYP-D3 has eliminated some major flaws in BDE calculations. However, both B3LYP and B3LYP-D3 performed only moderately well. Although Kruse et al suggested using larger basis sets, such as def2-TZVP or 6-311G(2df,2p), this did not help in our case when the 6-311++G(3d2f,2df,2p) basis set was used, as previously mentioned in Section 2.

The overall performance of all functionals employed in this work is depicted in Figure 4. The figure shows the MAPE for all DFT functionals in addition to the MP2 and CCSD(T) levels. As mentioned earlier, the largest errors were detected for the methods (MP2 and CCSD(T)), followed by the popular TPSSH and B3LYP. The functionals B97-D3, HSEH1PBE, BHandH, and APFD produced errors of roughly 5%. This is consistent with previous studies that found such functionals to perform moderately [27, 31]. We are, however, surprised by the moderate performance of Grimme's B97-D3, which employs one of the most accurate treatments of dispersion in chemical calculations [27, 31, 73]. This again agrees with the moderate performance of the B3LYP-D3 functional discussed earlier. It is worth noting that tellurium compounds have caused the majority of the errors in the B97-D3 functional (cf. Table 4). The developers of functional should take note of this and look into it.

As seen in Figure 4, the best functionals are MN12-SX, MN15-L, B3P86 and M06-2X. There are two significant points to be made here: (a) the top performing functionals belong to the highest levels in the Jacob's ladder; and (b) the functionals MN12-SX, B3P86, and M06-2X belong to level 4 in the Jacob's ladder, while the MN15-L functional belong to level 3. The fact that the performance of DFT functionals follows the order of the Jacob's ladder is consistent with the general trend that has recently been observed in several benchmarking studies [26, 27, 31]. The second observation is that four of the top performers belong to the Minnesota group. The excellent performance of the Minnesota group of functionals is also in agreement with previous benchmarking studies [2, 26, 27, 31, 33]. The efficiency of the Minnesota functionals, and the M06-2X in particular, is attributed to the fact that it is well parametrized for nonmetals [22, 37]. The accuracy of the B3P86 functional, an improved version of the 1986 Becke's one, is grabbing interest. In a study by Lazarou et al., the B3P86 functional demonstrated excellent performance in predicting BDE for halogenated hydrocarbons [68].

As mentioned in the Introduction section, the main goal of this work is to provide a reliable method to compute BDE for the fifth-row elements, when such values are poorly measured or validated. The BDE of this work's set of compounds were estimated and averaged using the best performing

TABLE 4 Absolute percentage errors for the bond dissociation energies at different level of theory.

	APFD	B3LYP	B3LYP-D3	B3P86	B97-D3	BhandH	HSEH1PBE	M06-2X	MN12-SX	MN15-L	TPSSH	MP2	CCSD(T)	Mean error	STD
CH_3CH_3	1.3	5.5	4.5	0.7	3.9	9.2	2.1	1.1	3.9	2.2	6.9	1.3	7.0	3.8	2.8
CH_3Cl	2.9	6.8	6.1	1.0	4.2	6.2	2.8	0.6	2.6	0.2	5.1	6.3	12.7	4.3	3.5
CH_3F	2.6	2.7	2.3	0.4	0.3	4.9	3.0	0.1	2.1	1.0	3.4	0.1	7.8	2.4	2.3
CH_3NO_2	5.6	10.4	8.1	3.8	11.6	-	5.5	2.3	8.1	3.8	13.0	3.1	8.9	6.9	4.1
H_2O	3.5	2.8	2.8	0.4	0.3	1.1	4.1	1.8	0.8	1.6	3.9	3.2	7.8	2.6	2.1
NH_3	2.3	1.8	1.7	1.5	0.2	3.6	2.8	0.2	2.8	0.7	2.7	3.6	7.0	2.4	1.9
PH_3	4.9	3.5	3.3	0.6	2.2	0.7	5.5	3.3	1.6	0.4	1.4	11.2	10.6	3.8	3.7
SF_6	5.4	12.8	12.2	5.1	14.0	11.8	7.2	2.0	4.1	7.7	10.5	1.5	7.9	7.5	4.1
TMA	4.1	10.9	7.9	4.4	7.9	10.3	5.7	2.5	1.9	2.4	11.7	4.1	7.9	6.2	3.5
TriMS (Me loss)	2.0	0.0	0.8	1.3	1.0	3.8	3.3	1.0	4.4	1.8	1.1	5.6	4.2	2.5	1.7
TriMS (H loss)	8.4	12.2	10.3	8.7	11.8	1.4	9.8	6.2	1.2	6.9	13.0	7.7	11.8	8.3	3.9
In_2F_6	6.9	4.2	3.8	3.8	1.2	4.1	7.4	1.9	1.4	3.7	8.3	0.3	6.8	4.2	2.7
$InCl_3$	5.4	7.6	6.6	3.9	5.5	0.3	6.1	2.3	3.1	4.0	7.1	8.3	12.5	5.5	3.2
InH_3	2.7	2.2	2.4	3.4	6.5	1.4	3.7	4.5	8.3	8.9	2.4	9.7	8.0	5.1	3.0
$InMe_3$	3.6	5.5	4.1	1.6	1.8	5.4	4.8	-	8.6	1.4	7.9	5.0	8.7	4.9	2.9
$InSb_2$	-	-		-	-	-	-	-	-	-	-	-	-	-	-
$SnCl_4$	4.2	10.5	8.3	4.2	9.1	4.0	5.8	3.2	2.3	6.8	8.4	4.3	9.5	6.0	2.8
SnH_4	4.4	0.5	0.2	0.6	2.9	0.4	5.4	3.3	6.6	3.7	0.7	8.6	7.3	3.7	2.8
$SnMe_4$	8.0	12.2	10.2	7.8	9.1	1.1	9.9	2.0	3.1	8.5	13.8	7.3	11.8	7.9	4.0
SnTriMeH	6.4	3.6	3.2	1.7	2.2	1.4	7.5	0.3	2.2	0.2	2.8	11.6	9.5	4.1	3.8
$SbCl_5$	-	-		-	-	-	-	-	-	-	-	-	-	-	-
SbH_3	5.9	2.8	2.5	0.4	2.5	2.4	6.8	0.8	4.6	0.3	1.3	16.1	12.6	4.7	5.0
$SbMe_5$	-	-		-	-	-	-	-	-	-	-	-	-	-	-
Te_2	6.2	9.2	9.2	2.0	13.6	12.8	5.4	1.7	8.7	2.6	7.8	-	-	7.0	4.7
$TeCl_4$	-	-		-	-	-	-	-	-	-	-	-	-	-	-
I_2	6.3	8.7	8.9	12.0	14.6	9.5	5.5	-	-	-	10.5	7.3	3.1	8.6	4.9
$TeMe_2$	-	-		-	13.3	9.7	-	6.0	6.5	-		21.8	25.1	13.7	9.0
HI	0.0	1.2	1.2	5.1	7.0	2.4	0.6	1.6	11.0	6.1	2.9	14.8	10.5	5.3	4.7
I_2	-	-		11.6	1.7	-	-	7.3	-	5.2	14.9			8.1	5.2
ICH_2Cl	7.6	15.9	14.0	7.3	4.7	2.6	8.7	0.3	6.2	9.3	11.9	16.9	19.7	9.2	5.9
ICl	-	-		-	-	-	-	-	-	-	-	-	-	-	-
ICN	1.6	3.6	2.9	2.3	2.4	9.7	1.1	5.7	10.6	2.1	2.8	21.3	7.2	5.9	5.8
IF	12.1	9.9	9.9	6.4	1.1	9.4	12.5	6.5	0.9	8.4	9.1	3.8	14.2	7.8	4.3

TABLE 4 (Continued)

	APFD	B3LYP	B3LYP-D3	B3P86	B97-D3	BhandH	HSEH1PBE	M06-2X	MN12-SX	MN15-L	TPSSH	MP2	CCSD(T)	Mean error	STD
Mean error	4.8	6.4	5.7	3.8	5.6	5.0	5.5	2.6	4.5	3.8	6.9	7.9	10.0		
STD	2.8	4.6	4.0	3.4	4.8	4.0	3.1	2.2	3.2	3.1	4.6	6.2	5.1		
RMSE	19.9	27.2	24.1	16.7	22.9	21.9	22.3	12.1	19.2	18.4	27.4	39.8	41.0		
Pearson's correlation (*R*)	0.9881	0.9761	0.9800	0.9828	0.9637	0.9735	0.9872	0.9887	0.9868	0.9762	0.9708	0.9557	0.9787		

Note: Empty fields represent omitted outliers.

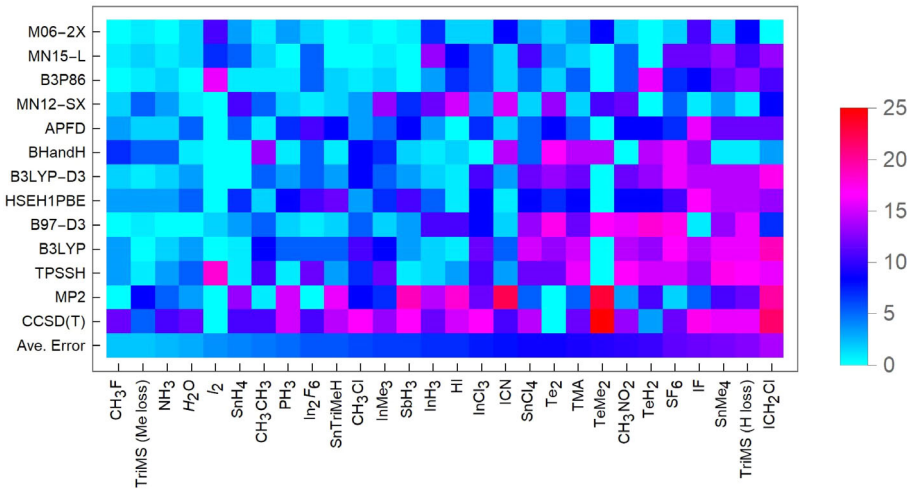

FIGURE 3 Absolute percentage errors for the bond dissociation energies at different levels of theory, after excluding the outliers.

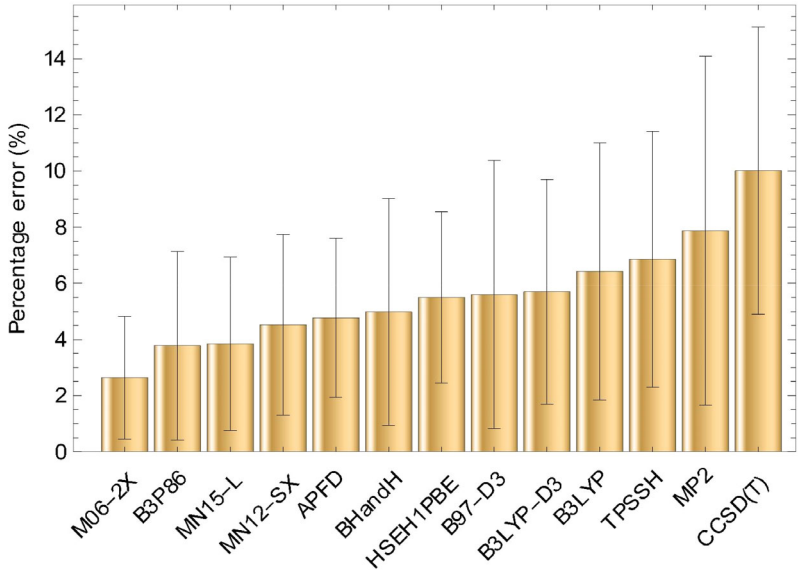

FIGURE 4 Mean absolute percentage error (MAPE) for different DFT functionals and ab-initio methods.

functionals, MN12-SX, MN15-L, B3P86, and M06-2X. The results are shown in Table 5 along with the experimental values as a baseline for comparison. The absolute percentage errors shown in the table correspond to the deviation from the experimental values. The compounds, $TeCl_4$, $SbCl_5$, $InSb_2$, $Sb(CH_3)_5$, and ICl, have demonstrated large errors in their BDE values and are highlighted in Table 5. The high inaccuracies are caused by the erroneous experimental value, as we discussed earlier. Otherwise, the results of Table 5 are mostly acceptable with many errors being less than 1%. Some exclusions include InH_3, SbH_4, HI, and the H-loss in TriMS. These cases involve the hemolytic rupture of the M—H bond, where M is a heavy element. In a study by Moltved et al., the metal hydride problem was investigated under different functionals [22]. According to the study, the inaccuracy in the BDE of the M—H bond is largely caused by the self-interaction error (SIE). The error represents the failure of density functionals ignores the exact cancellation of the exchange and coulomb integrals for electrons. Based on Moltved's study, the HF and post-HF methods, such as CCSD(T), are not suitable for describing the M—H bond [22]. In this work, some of the large errors in measuring the BDE of the M—H bond were even created by the top-performing functionals, which very well described the electron density. Indeed, this is a matter that the developers of functional should look into.

Finally, accuracy in computational calculations is typically acceptable to be on the order of 1 kcal (4.184 kJ) [17, 30]. According to our results in Table 5, the deviations from the experimental value are within the range of 1–4 kJ/mol (excluding the outliers). On the basis of these findings, we advise choosing one of the functionalities with the best performance, or a subset of them, and using the mean value of their scores in any future calculations of the heavy elements in the fifth row, paying close attention to the M—H bond dissociation.

TABLE 5 The average BDE (kJ/mol) obtained with best methods: MN12-SX, MN15-L, B3P86, and M06-2X.

	Exp. BDE (kJ/Mol)	BDE calculated by best four methods (kJ/Mol)	Absolute percentage error (100%)
CH_3CH_3	377.4	376.3	0.3
CH_3Cl	350.2	348.4	0.5
CH_3F	460.2	461.7	0.3
CH_3NO_2	260.7	257.4	1.3
H_2O	497.1	493.5	0.7
NH_3	450.1	452.0	0.4
PH_3	351.0	347.9	0.9
SF_6	391.6	391.4	0.1
TMA	328.9	324.1	1.5
TriMS (Me loss)	387.0	391.1	1.1
TriMS (H loss)	396.2	370.3	6.5
In_2F_6	506.0	495.7	2.0
$InCl_3$	364.8	361.0	1.0
InH_3	295.8	316.7	7.1
$InMe_3$	269.0	279.1	3.8
$InSb_2$	279.1	204.4	26.8
$SnCl_4$	305.0	297.1	2.6
SnH_4	346.0	360.3	4.1
$SnMe_4$	295.0	285.8	3.1
SnTriMeH	326.4	326.0	0.1
$SbCl_5$	248.0	154.9	37.5
SbH_3	288.3	293.1	1.7
$SbMe_5$	255.0	194.2	23.8
Te_2	257.6	269.1	4.5
$TeCl_4$	310.0	152.8	50.7
TeH_2	272.0	309.6	13.8
$TeMe_2$	276.0	246.2	10.8
HI	298.3	317.5	6.4
I_2	152.3	153.7	0.9
ICH_2Cl	221.8	217.3	2.0
ICl	211.3	181.5	14.1
ICN	320.1	332.9	4.0
IF	271.5	261.3	3.8

4 | CONCLUSIONS

Compounds containing fifth-row elements, with their heavy nuclei and large number of electrons, have posed a challenge to computational chemistry. Although some BDEs of these compounds have been determined either experimentally or theoretically, validation of these values remains incomplete. In this study, we employed ab-initio methods to accurately calculate the BDE of compounds containing fifth-row elements. To ensure robustness of the benchmark study, we tested the set of compounds including common small molecules such as H_2O, NH_3, and PH_3. We employed popular DFT functionals, as well as the well-known MP2 and CCSD(T) techniques. Using systematic statistical analysis, we obtained final average errors for each method, which enabled us to assess their performance.

Our findings revealed that the accuracy of the DFT functionals followed the general order of the Jacob's ladder. Notably, the widely used functionals such as B3LYP, APFD, and B97-D3 performed poorly in estimating the BDE of the tested compounds, with B3LYP even failing to predict BDEs of some common small organic compounds containing silicon. The addition of dispersion correction (D3) to B3LYP only slightly improved the results. Interestingly, the MP2 and CCSD(T) techniques demonstrated unexpected poor performance when applied to the fifth-row

elements (In—I). This can be attributed to the incomplete treatment of the electron correlation problem in these complex and heavy structures. Additionally, the relativistic effects, choice of basis set configuration used in these methods might contributed to their underperformance.

The study identified the Minnesota group functionals, MN12-SX, MN15-L, and M06-2X, as well as the B3P86 functional, as top-performing functionals, which were well parametrized for nonmetal elements. The performance of these functionals is in line with their hierarchy in the Jacob's ladder. Our results also showed that most of the errors in this study were associated with compounds containing an M—H bond, as well as those containing tellurium compounds. Further investigation is needed to better understand the underlying causes of these errors and to address them.

This benchmark study has promising applications in a variety of fields beyond chemistry, including the development of catalysis, protein folding, and energy storage and generation. The ability to accurately determine bond dissociation energies of compounds containing specific elements is critical for advancing research in these areas, and this work offers a powerful tool to achieve this goal. Overall, this work has significant implications for a wide range of scientific fields and has the potential to drive new discoveries and advancements in these areas.

AUTHOR CONTRIBUTIONS

The authors confirm contribution to the paper as follows: study conception and design: Ismail Badran, Nashaat N. Nassar; theoretical calculations and modeling: Ismail Badran; data analysis and validation, Ismail Badran, Kotaybah Hashlamoun; draft manuscript preparation: Ismail Badran, Kotaybah Hashlamoun, Nashaat N. Nassar. All authors reviewed the results and approved the final version of the manuscript.

ACKNOWLEDGMENTS

The authors are grateful to the Department of Chemistry and the Faculty of Science at An-Najah National University, the Department of Chemical and Petroleum Engineering, University of Calgary, the Natural Sciences and Engineering Research Council of Canada (NSERC) for their support to this project. Thanks to the Digital Research Alliance of Canada (Compete Canada). The authors also thankful to Dr. K. Dergham for his consultations during the statistical analysis of this work.

CONFLICT OF INTEREST STATEMENT

The authors declare that they have no known competing financial interests or personal relationships that could have appeared to influence the work reported in this paper.

DATA AVAILABILITY STATEMENT

The data that support the findings of this study are openly available in Mendeley Data, V1 at https://www.doi.org/10.17632/vvbcfvwrzx.2.

ORCID

Ismail Badran https://orcid.org/0000-0003-1423-7124
Nashaat N. Nassar https://orcid.org/0000-0001-9014-542X

REFERENCES

[1] P. C. St. John, Y. Guan, Y. Kim, S. Kim, R. S. Paton, *Nat. Commun.* **2020**, *11*, 2328.
[2] X. Li, X. Xu, X. You, D. G. Truhlar, *J. Phys. Chem. A* **2016**, *120*, 4025.
[3] L. Cheng, J. Gauss, B. Ruscic, P. B. Armentrout, J. F. Stanton, *J. Chem. Theory Comput.* **2017**, *13*, 1044.
[4] M. Kaupp, D. Danovich, S. Shaik, *Coord. Chem. Rev.* **2017**, *344*, 355.
[5] N. Kosar, K. Ayub, M. A. Gilani, F. Shah, T. Mahmood, *Int. J. Quantum Chem.* **2020**, *120*, e26106.
[6] L. de Azevedo Santos, T. C. Ramalho, T. A. Hamlin, F. M. Bickelhaupt, *J. Comput. Chem.* **2021**, *42*, 688.
[7] N. Kosar, K. Ayub, M. A. Gilani, T. Mahmood, *J. Mol. Model.* **2019**, *25*, 47.
[8] S. Jana, H. Myneni, S. Śmiga, L. A. Constantin, P. Samal, *J. Chem. Phys.* **2021**, *155*, 114102.
[9] J. Tao, J. P. Perdew, V. N. Staroverov, G. E. Scuseria, *Phys. Rev. Lett.* **2003**, *91*, 146401.
[10] Y. Zhao, D. G. Truhlar, *Chem. Phys. Lett.* **2011**, *502*, 1.
[11] A. Tafvizi, L. A. Mirny, A. M. van Oijen, *ChemPhysChem* **2011**, *12*, 1481.
[12] M. M. Gromiha, R. Nagarajan, in *Advances in Protein Chemistry and Structural Biology*, Vol. 91 (Ed: R. Donev), Academic Press, Swansea, United Kingdom **2013**, p. 65.
[13] R. A. Van Santen, M. Neurock, S. G. Shetty, *Chem. Rev.* **2010**, *110*, 2005.
[14] R. Al-Akbari, M. Razi, I. Badran, N. N. Nassar, *React. Chem. Eng.* **2023**, *8*, 1083.
[15] Y.-R. Luo, *Comprehensive Handbook of Chemical Bond Energies*, CRC Press, Boca Raton, Florida, USA **2007**.
[16] I. N. Levine, *Quantum Chemistry*, 7th ed., Pearson Prentice Hall Upper Saddle River, NJ, USA **2014**.
[17] J. Harvey, *Computational Chemistry*, Oxford University Press, London, UK **2018**.
[18] C. J. Cramer, *Essentials of Computational Chemistry: Theories and Models*, John Wiley & Sons, NY, USA **2013**.
[19] I. Badran, A. Rauk, Y. J. Shi, *J. Phys. Chem. A* **2012**, *116*, 11806.
[20] J. Shee, M. Loipersberger, A. Rettig, J. Lee, M. Head-Gordon, *J. Phys. Chem. Lett.* **2021**, *12*, 12084.
[21] J. Shee, B. Rudshteyn, E. J. Arthur, S. Zhang, D. R. Reichman, R. A. Friesner, *J. Chem. Theory Comput.* **2019**, *15*, 2346.
[22] K. A. Moltved, K. P. Kepp, *J. Phys. Chem. A* **2019**, *123*, 2888.

[23] T. B. Adler, G. Knizia, H.-J. Werner, *J. Chem. Phys.* **2007**, *127*, 221106.
[24] H.-J. Werner, T. B. Adler, F. R. Manby, *J. Chem. Phys.* **2007**, *126*, 164102.
[25] X. Xu, W. A. Goddard, *J. Phys. Chem. A* **2004**, *108*, 8495.
[26] R. Peverati, D. G. Truhlar, *Philosophical Transactions of the Royal Society A: Mathematical, Physical and Engineering Sciences* **2011**, *2014*, 20120476.
[27] L. Goerigk, A. Hansen, C. Bauer, S. Ehrlich, A. Najibi, S. Grimme, *PCCP* **2017**, *19*, 32184.
[28] M. Korth, S. Grimme, *J. Chem. Theory Comput.* **2009**, *5*, 993.
[29] H. Kruse, L. Goerigk, S. Grimme, *J. Org. Chem.* **2012**, *77*, 10824.
[30] J. P. Perdew, A. Ruzsinszky, J. Tao, V. N. Staroverov, G. E. Scuseria, G. I. Csonka, *J. Chem. Phys.* **2005**, *123*, 62201.
[31] N. Mardirossian, M. Head-Gordon, *Mol. Phys.* **2017**, *115*, 2315.
[32] P. J. Stephens, F. J. Devlin, C. F. Chabalowski, M. J. Frisch, *J. Phys. Chem. A* **1994**, *98*, 11623.
[33] L. Goerigk, S. Grimme, *Phys. Chem. Chem. Phys.* **2011**, *13*, 6670.
[34] I. Badran, Z. Talie, *Iran. J. Chem. Chem. Eng. (IJCCE)* **2021**, *40*, 1490.
[35] L. Goerigk, N. Mehta, *Aust. J. Chem.* **2019**, *72*, 563.
[36] H. S. Yu, X. He, D. G. Truhlar, *J. Chem. Theory Comput.* **2016**, *12*, 1280.
[37] Y. Zhao, D. G. Truhlar, *Theor. Chem. Acc.* **2008**, *120*, 215.
[38] R. Peverati, D. G. Truhlar, *PCCP* **2012**, *14*, 13171.
[39] L. P. Viegas, *Int. J. Quantum Chem.* **2017**, *117*, e25381.
[40] L. N. Anderson, F. W. Aquino, A. E. Raeber, X. Chen, B. M. Wong, *J. Chem. Theory Comput.* **2018**, *14*, 180.
[41] G. S. James, *Lange's Handbook of Chemistry*, New York, NY, USA, MCGraw-Hill **2005**.
[42] J. P. Merrick, D. Moran, L. Radom, *J. Phys. Chem. A* **2007**, *111*, 11683.
[43] E. R. Johnson, O. J. Clarkin, G. A. DiLabio, *J. Phys. Chem. A* **2003**, *107*, 9953.
[44] I. Badran, A. Rauk, Y. Shi, *J. Phys. Chem. A* **2019**, *123*, 1749.
[45] T. H. Dunning Jr, P. J. Hay, in *Methods of Electronic Structure Theory*, Vol. 2 (Ed: H. F. Schaefer III), Plenum Press, New York, USA **1977**, p. 1.
[46] A. Austin, G. A. Petersson, M. J. Frisch, F. J. Dobek, G. Scalmani, K. Throssell, *J. Chem. Theory Comput.* **2012**, *8*, 4989.
[47] A. D. Becke, *J. Chem. Phys.* **1993**, *98*, 5648.
[48] J. P. Perdew, Y. Wang, *Phys. Rev. B: Condens. Matter* **1992**, *45*, 13244.
[49] S. Grimme, J. Antony, S. Ehrlich, H. Krieg, *J. Chem. Phys.* **2010**, *132*, 154104.
[50] S. Grimme, S. Ehrlich, L. Goerigk, *J. Comput. Chem.* **2011**, *32*, 1456.
[51] A. D. Becke, *J. Chem. Phys.* **1993**, *98*, 1372.
[52] J. Heyd, G. E. Scuseria, *J. Chem. Phys.* **2004**, *120*, 7274.
[53] A. V. Krukau, O. A. Vydrov, A. F. Izmaylov, G. E. Scuseria, *J. Chem. Phys.* **2006**, *125*, 224106.
[54] M. Head-Gordon, J. A. Pople, M. J. Frisch, *Chem. Phys. Lett.* **1988**, *153*, 503.
[55] J. S. Binkley, J. A. Pople, *Int. J. Quantum Chem* **1975**, *9*, 229.
[56] G. E. Scuseria, C. L. Janssen, H. F. Schaefer III, *Chem. Phys.* **1988**, *89*, 7382.
[57] G. D. Purvis III, R. J. Bartlett, *J. Chem. Phys.* **1982**, *76*, 1910.
[58] M. J. Frisch, G. W. Trucks, H. B. Schlegel, G. E. Scuseria, M. A. Robb, J. R. Cheeseman, G. Scalmani, V. Barone, G. A. Petersson, H. Nakatsuji, X. Li, M. Caricato, A. V. Marenich, J. Bloino, B. G. Janesko, R. Gomperts, B. Mennucci, H. P. Hratchian, J. V. Ortiz, A. F. Izmaylov, J. L. Sonnenberg, Williams, F. Ding, F. Lipparini, F. Egidi, J. Goings, B. Peng, A. Petrone, T. Henderson, D. Ranasinghe, V. G. Zakrzewski, J. Gao, N. Rega, G. Zheng, W. Liang, M. Hada, M. Ehara, K. Toyota, R. Fukuda, J. Hasegawa, M. Ishida, T. Nakajima, Y. Honda, O. Kitao, H. Nakai, T. Vreven, K. Throssell, J. A. Montgomery Jr., J. E. Peralta, F. Ogliaro, M. J. Bearpark, J. J. Heyd, E. N. Brothers, K. N. Kudin, V. N. Staroverov, T. A. Keith, R. Kobayashi, J. Normand, K. Raghavachari, A. P. Rendell, J. C. Burant, S. S. Iyengar, J. Tomasi, M. Cossi, J. M. Millam, M. Klene, C. Adamo, R. Cammi, J. W. Ochterski, R. L. Martin, K. Morokuma, O. Farkas, J. B. Foresman, D. J. Fox, Gaussian 16 Rev. C.01. Wallingford, CT, USA. **2016**.
[59] R. Dennington, T. Keith, J. Millam, *GaussView, Version 6*, Semichem Inc., Shawnee Mission, KS **2016**.
[60] W. Mendenhall, T. Sincich, *Statistics for Engineering and the Sciences*, CRC, Taylor and Francis Group, UK **2016**.
[61] N. Kosar, K. Ayub, M. A. Gilani, S. Muhammad, T. Mahmood, *ACS Omega* **2022**, *7*, 20800.
[62] C. C. Aggarwal, *Outlier Analysis*, Springer, Cham, New York, USA **2017**.
[63] F. Cribari-Neto, A. Zeileis, *J. Stat. Softw.* **2010**, *34*, 1.
[64] Wolfram Research, Inc, *Mathematica*, Wolfram Research, Inc., Champaign, Illinois **2022**.
[65] Ma, Z.; Zaera, F. *Encyclopedia of Inorganic Chemistry*, John Wiley & Sons, Inc, New York, USA **2006**.
[66] W. M. Haynes, *CRC Handbook of Chemistry and Physics*, CRC Press, Boca Raton, Florida, USA **2014**.
[67] T. McAllister, *J. Cryst. Growth* **1989**, *96*, 552.
[68] Y. G. Lazarou, A. V. Prosmitis, V. C. Papadimitriou, P. Papagiannakopoulos, *J. Phys. Chem. A* **2001**, *105*, 6729.
[69] B. Chan, A. Karton, K. Raghavachari, *J. Chem. Theory Comput.* **2019**, *15*, 4478.
[70] B. Chan, *J. Chem. Theory Comput.* **2021**, *17*, 5704.
[71] B. Chan, A. Karton, *J. Comput. Chem.* **2022**, *43*, 1394.
[72] Z. Fang, M. Vasiliu, K. A. Peterson, D. A. Dixon, *J. Chem. Theory Comput.* **2017**, *13*, 1057.
[73] Y. Zheng, W. Zheng, J. Wang, H. Chang, D. Zhu, *J. Phys. Chem. A* **2018**, *122*, 2764.

How to cite this article: I. Badran, K. Hashlamoun, N. N. Nassar, *Int. J. Quantum Chem.* **2023**, e27222. https://doi.org/10.1002/qua.27222